Supporting Information

Shape-Tailoring of CuPd Nanocrystals by Single Parameter Adjustment for Enhancement of Electrocatalytic Activity

Li Zhang, Fei Hou, and Yiwei Tan*

State Key Laboratory of Materials-Oriented Chemical Engineering, School of Chemistry and Chemical Engineering, Nanjing University of Technology, Nanjing 210009, China, Email: ytan@njut.edu.cn

Experimental Section

Materials: All reagents were commercially available and used as received. $Pd(acac)_2$ (Pd 34.7%), $Cu(acac)_2$ (98%), formanilide (98%), *o*-anisidine (99%), aniline (99%), and 1-octadecene (90%) were purchased from Alfa Aesar. Oleic acid (90%) and oleylamine (70%) were purchased from Sigma-Aldrich.

Synthesis: All the syntheses were carried out through a standard airless procedure under vigorous magnetic stirring. In a typical experiment, $Pd(acac)_2$, $Cu(acac)_2$, and formanilide with their concentrations in the final solution described in the main text were mixed together with oleylamine (2.4 mL), oleic acid (0.6 mL), and 1-octadecene (2.0 mL) at 60 °C in a 50 mL three-neck round-bottom flask equipped with a condenser and attached to a Schlenk line. The reaction system was purged of air by three cycles of evacuation and followed by blowing a nitrogen stream. The mixture was heated to 200 °C at a heating rate of ~ 20 °C/min and then was refluxed for 20 min at this temperature under a nitrogen stream. Subsequently, the black solution was cooled down to room temperature naturally by removing the reaction flask from the heating mantle. The CuPd alloy nanocrystals were isolated by precipitating the colloids from the final reaction solution using 30 mL of ethanol. The precipitates were washed with 10 mL of ethanol again. Finally, the precipitates were redissolved in hexane for further characterization.

Characterization: A JEOL-2100 transmission electron microscope (TEM) operated at 200 kV was used for traditional TEM imaging. High resolution TEM (HRTEM) images, selected area electron diffraction (SAED) pattern, and energy-dispersive X-ray spectroscopy (EDS) were acquired on a FEI Tecnai G2 F20 S-Twin TEM operated at 200 kV. Scanning transmission electron microscopy (STEM), EDS line scan profiles, and elemental maps were carried out using the high-angle annular dark field (HAADF) mode on the same HRTEM. Samples for TEM or HRTEM characterization were prepared by placing one drop of nanoparticle solution in hexane onto 300-mesh carbon-coated copper or nickel grids, respectively. Element analyses for the composition of the particles were carried out with EDS and ICP-AES (Teledyne-Leeman Laboratories, Prodigy, high dispersion ICP). A Hitachi S-4800 field-emission scanning electron microscope (FESEM) operated at 5 kV was used for HRSEM imaging. To identify the outline of the nanoparticles, the specimen was thoroughly washed with ethanol for several times to remove the adsorbed surfactants prior to SEM observation. XRD patterns were recorded on a Rigaku D/max-2500VL/PC diffractometer operated at 40 kV voltage and a 200 mA current with Cu Kα radiation.

Electrochemical Measurements: Electrochemical measurements were performed using a glassy carbon (GC) rotating disk electrode (RDE, Pine Research Instrumentation) connected to a CHI 660D electrochemical analyzer (CH Instruments, Chen-Hua Co., Shanghai, China) in a three-electrode glass cell at room temperature. A Ag/AgCl/KCl (3 M) or Hg/HgO electrode was used as the reference electrode, respectively. A Pt wire served as the counter electrode. The GC disk electrodes (5 mm diameter, 0.196 cm^2) acted as the substrate for the supported Pt/C or CuPd catalysts and were polished with 0.3 and 0.05 μm alumina slurries on a polishing cloth before each experiment. Following their polishing to a mirror-finish, the electrodes were cleaned in an ultrasonic bath (ethanol and then water) for 10 min and then were thoroughly rinsed with deionized water. All potentials were quoted versus the reversible hydrogen electrode (NHE). All water was Millipore ultrapure water (18.2 MΩ). For determining the electrochemically active surface areas (ECSA) of catalysts, cyclic voltammograms (CV) were run in a N_2-purged 0.10 M sulfuric acid solution at a scan rate of 50 mV/s. The ORR measurements were performed under oxygen purging in O_2-saturated 0.10 M sulfuric acid at a scan rate of 10 mV/s. The rotation rate of a RDE was set at 1600 rpm. To attain stable electrocatalytic performance, all the electrochemical data were recorded after the working electrodes achieved the steady state by continuous potential cycling prior to each activity measurement.

Preparation of Working Electrodes: For the commercial Pt/C catalyst (Johnson-Matthey, 20 wt%), an aqueous dispersion of Pt/C (1 mg/mL) was prepared and sonicated for 10 min. 3 μL of the dispersion was dropped onto the GC RDE. For the CuPd catalysts, the nanoparticles were further washed with ethanol for 5 times and then treated by UV light irradiation for 24 h in air to remove the organic surfactants before preparing the working electrodes.[1] Typically, TEM image of the treated CuPd nanocubes is shown in Figure S7. Subsequently, aqueous suspensions of 1 mg/mL CuPd catalyst were prepared by ultrasonication according to weighting and ICP-AES measurement and then 3 μL of each suspension is transferred onto the RDE to obtain the catalytic electrode. Upon drying in air for 2 h, the electrode was covered with 5 μL of a 0.10 wt% Nafion solution. After evaporation of water, the electrode was placed under vacuum for 0.5 h prior to measurement.

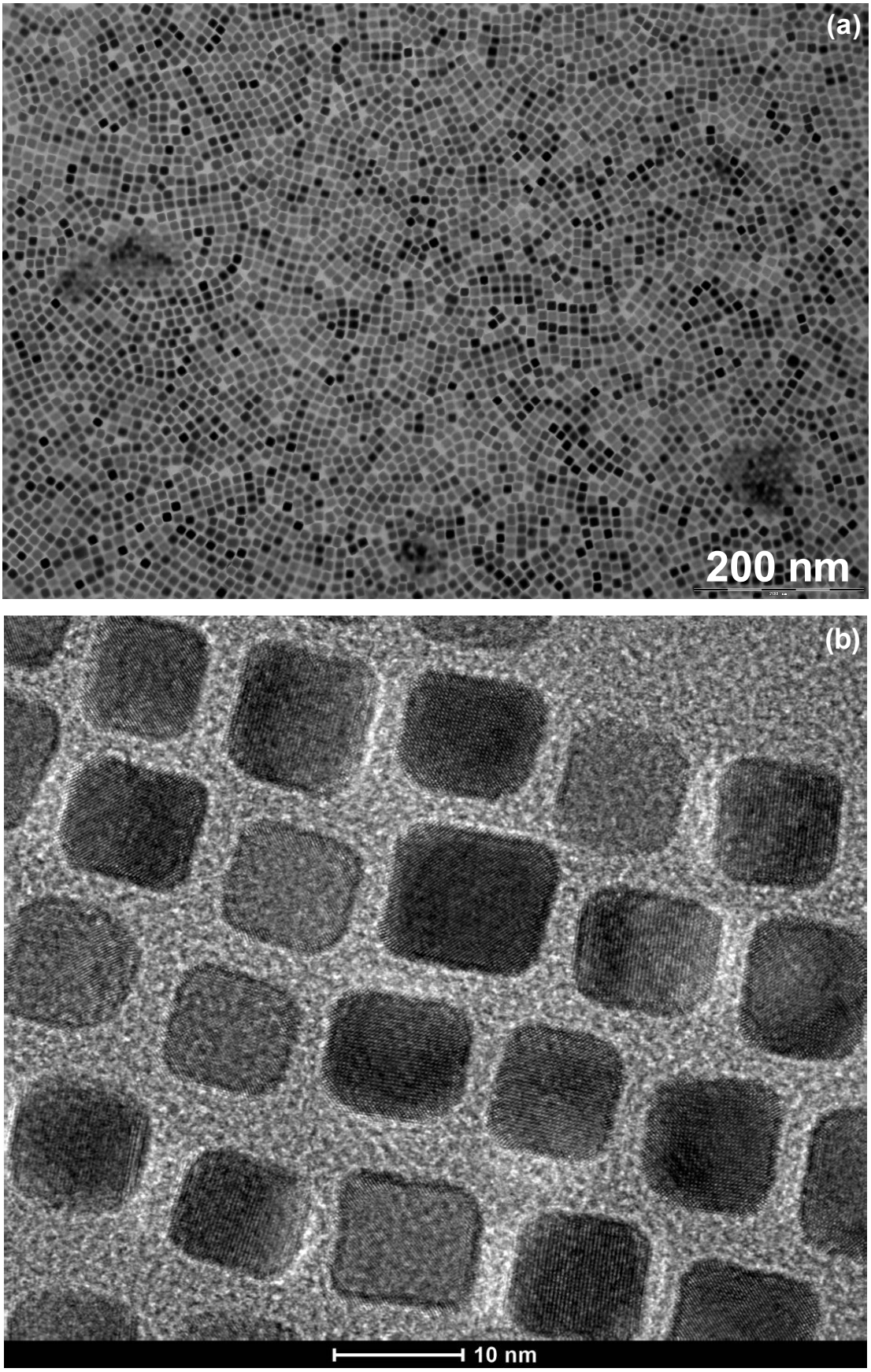

Figure S1. Large-area (a) TEM and (b) HRTEM images of CuPd nanocubes.

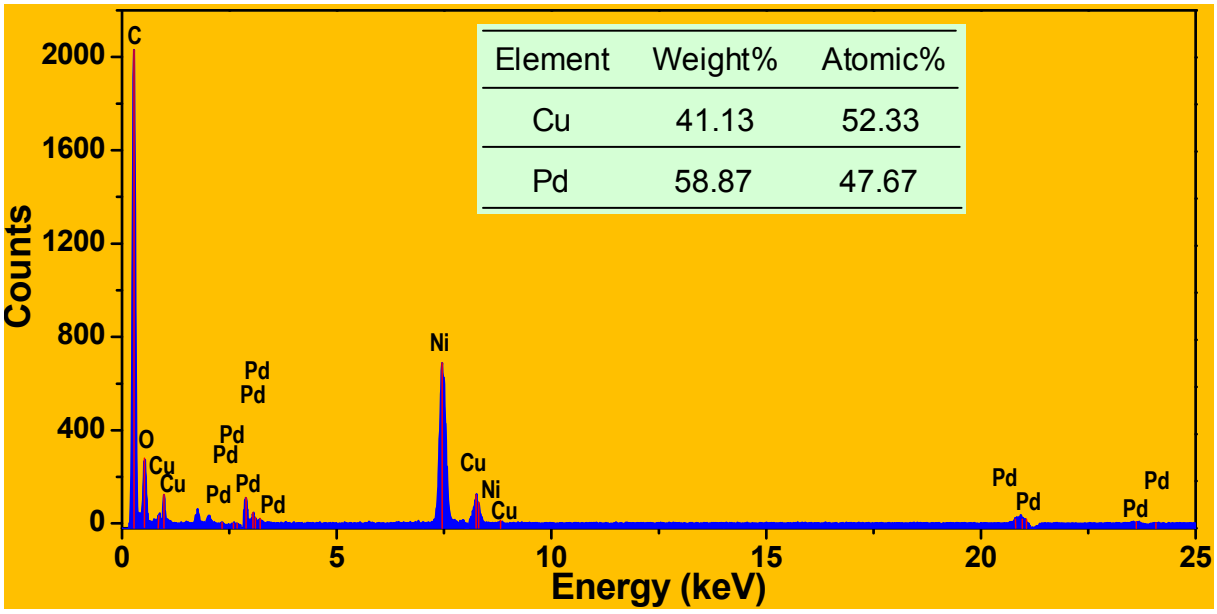

Figure S2. Energy-dispersive X-ray (EDX) spectra of cubic CuPd nanocrystals.

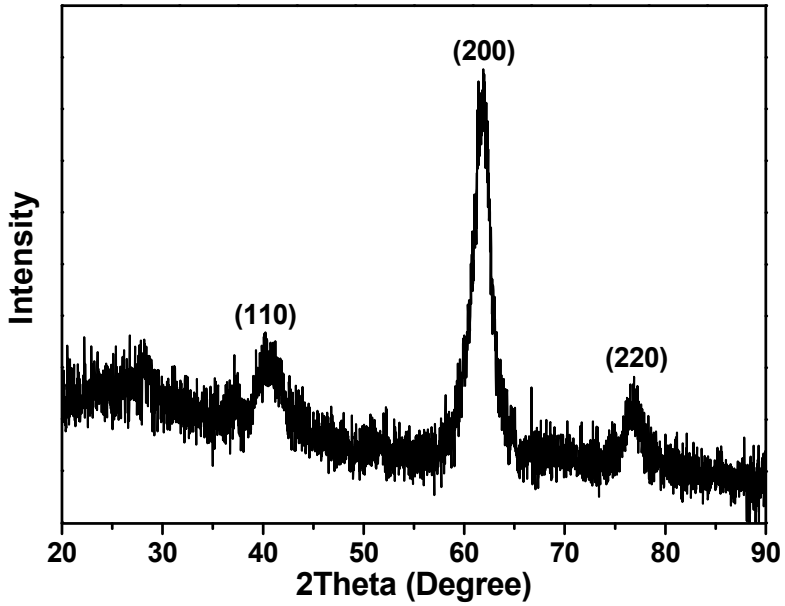

Figure S3. Powder XRD pattern of CuPd nanocubes.

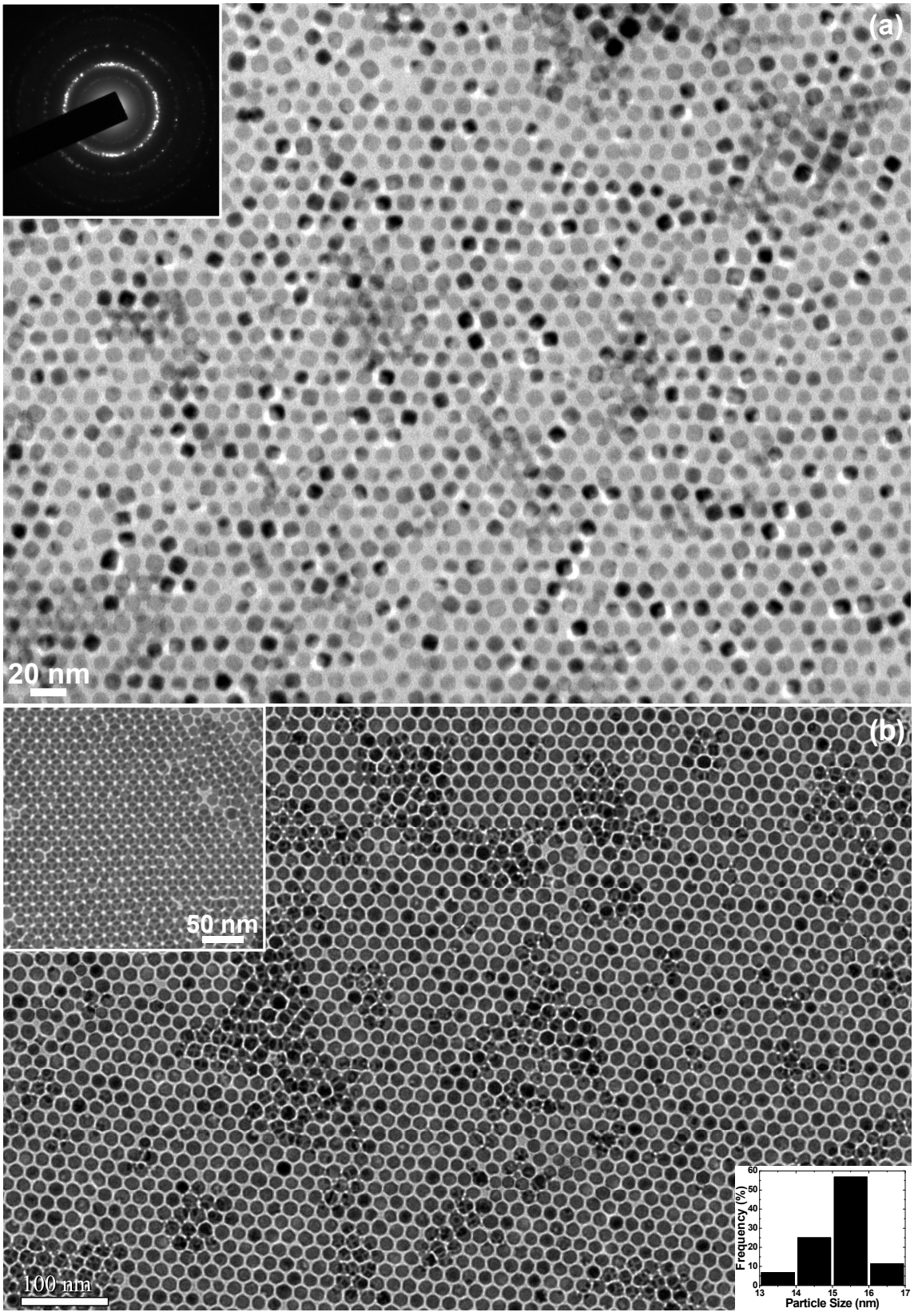
(a)
20 nm
(b)
50 nm
100 nm
Frequency (%)
Particle Size (nm)
0
10
20
30
40
50
60
13
14
15
16
17

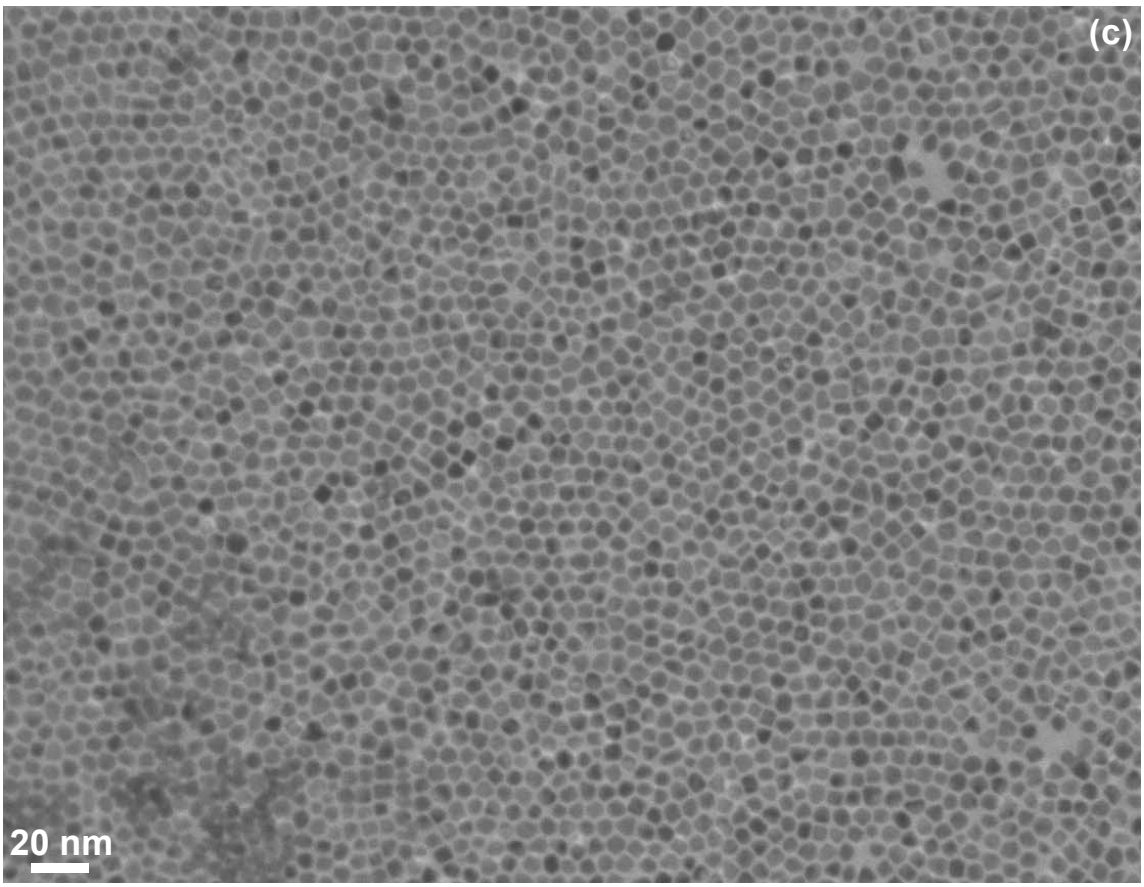

Figure S4. Large-area TEM images of the as-synthesized (a) truncated cubic, (b) cuboctahedral, and (c) irregular polyhedral CuPd nanocrystals. The insets: (a) a SAED pattern and (b) a bilayer hcp of cuboctahedral CuPd nanoparticles (top) and the corresponding size histogram (bottom).

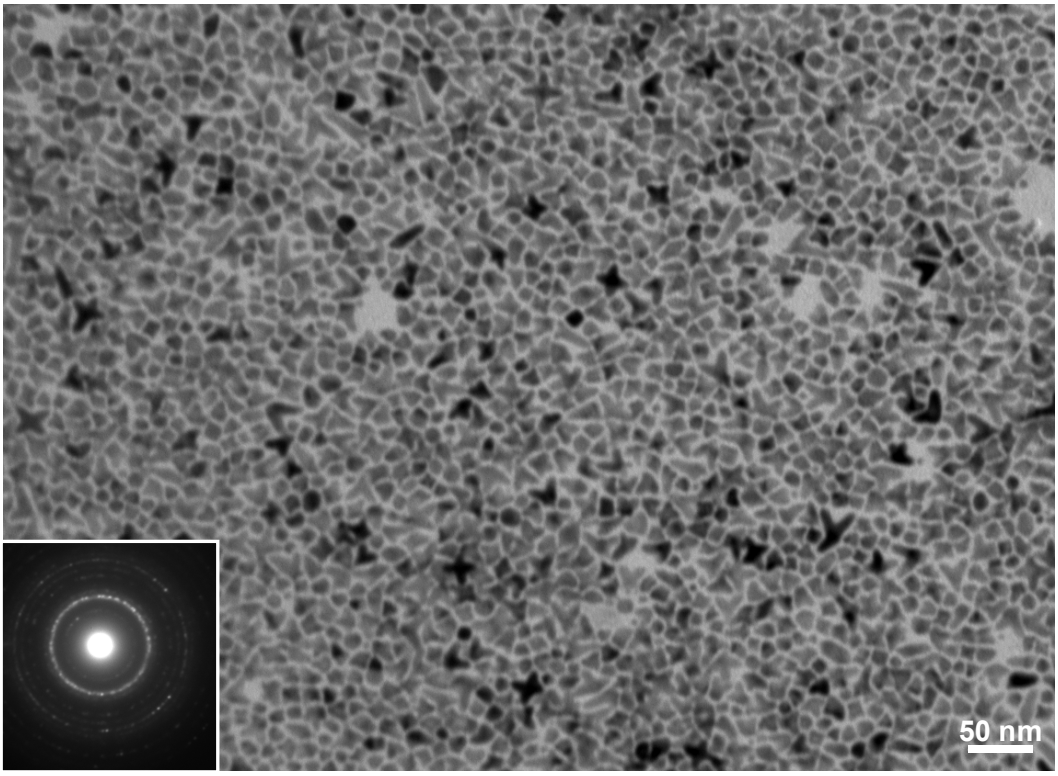

Figure S6. TEM image of branched (tetrapod-like) CuPd nanocrystals. The inset shows the corresponding SAED pattern.

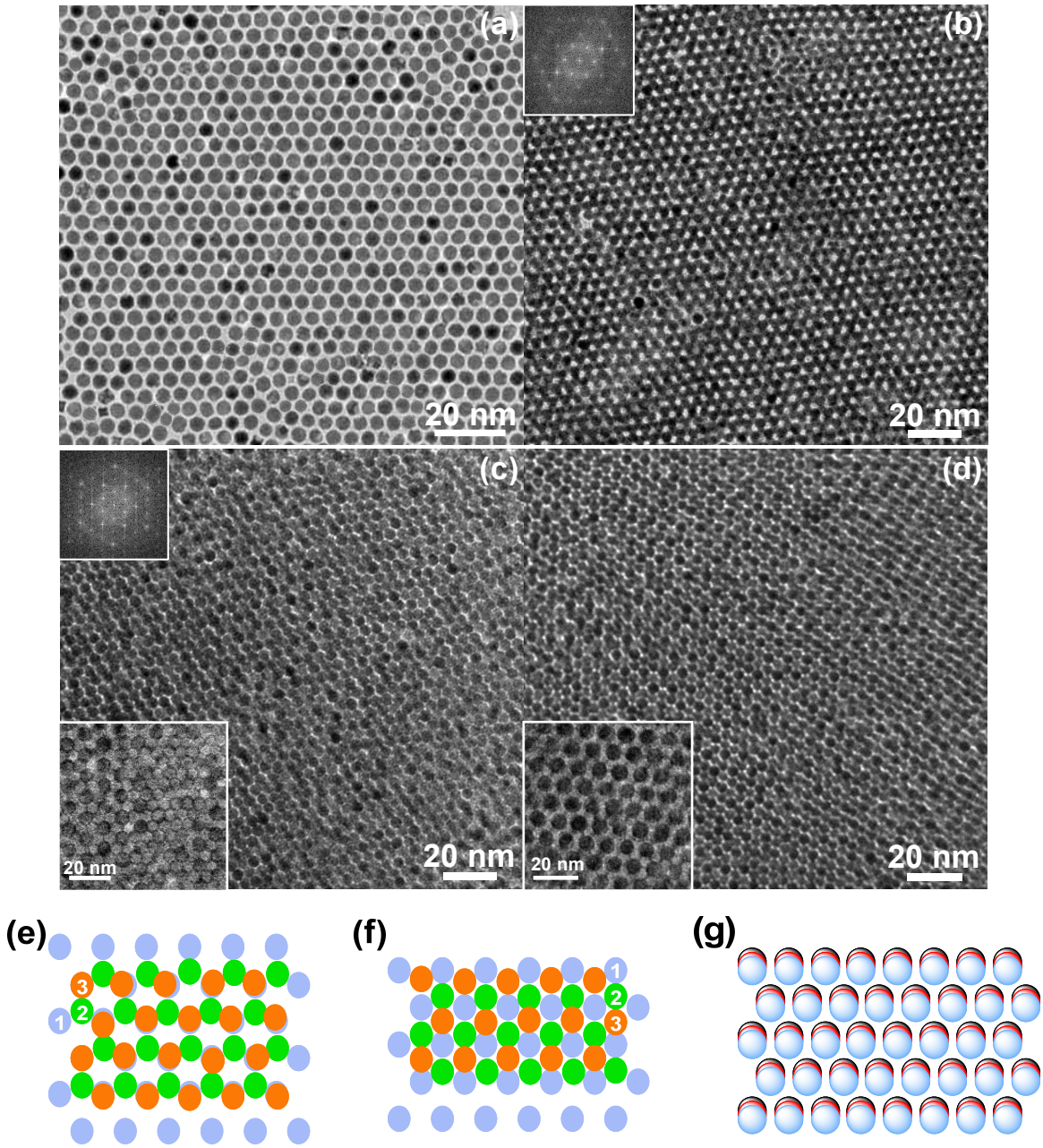

Figure S5. TEM images of (a–d) 3.8 nm CuPd nanoparticles prepared with aniline as the reductant. The nanoparticles self-assemble into (b) an hcp, (c) an [111] oriented fcc, and (d) a simple hexagonal 3D superlattice. The bottom insets in panel c and d exhibit TEM images of the same superlattice structure self-assembled from 6.6 nm CuPd nanoparticles prepared with *o*-anisidine as the reductant. The top insets in panel b and c present the corresponding FFT of the image. The cartoon schematically presents the self-assembled CuPd nanoparticle superlattices: (e) hcp and (f) fcc viewed along the [111] projection direction, (g) simple hexagonal superlattice viewed from the [001] direction.

To clearly understand the growth of the CuPd nanocubes and the shape evolution, a set of control experiments were carried out, in which aniline or *o*-anisidine was used as the reducing reagent while maintaining all other experimental parameters unchanged with respect to the preparation of nanocubes. In contrast, TEM observations reveal that monodisperse spherical CuPd nanoparticles are formed. The size analysis from TEM images illustrates that the use of aniline results in the formation of 3.8 nm CuPd nanoparticles, while the reduction reaction produces 6.6 nm CuPd nanoparticles if *o*-anisidine is utilized as the reductant (Figure S6). In view of the fact that the reduction potential of formaldehyde (0.85 V vs. a normal hydrogen electrode (NHE))[2] is lower than that of aniline (1.05 V vs. NHE),[3,4] we infer that a similar potential difference exists between formanilide and aniline because formanilide contains an aldehyde group as formaldehyde does while no exact reduction potential is known for formanilide at this point. At the same time, the aniline group of formanilide, by its electron donating effect in comparison with H atom of formaldehyde, increases

the electron density of the aldehyde group and hence, makes formanilide more easily oxidized. Therefore, an additional evidence is provided to support the underlying mechanism that the morphological evolution of CuPd nanocrystals is controlled by the reduction kinetics of the Cu and Pd cations.

The choice of a different concentration of formanilide enables the reaction to reach the relevant rate at which Cu and Pd atoms are favorably incorporated along certain directions through relaxation driven by different surface tensions of facets of CuPd nuclei. The same type and concentration of ligands provide an identical surfactant effect on the thermodynamic stabilization of growing various shaped CuPd nanocrystals at the same reaction temperature. The unique role played by formanilide is assumed to be its complexation with Cu^{2+} and Pd^{2+} to control reaction rate as well as to be ligand to enhance the ability to stabilize the {100} facets of CuPd nanocrystals with increasing its concentration.

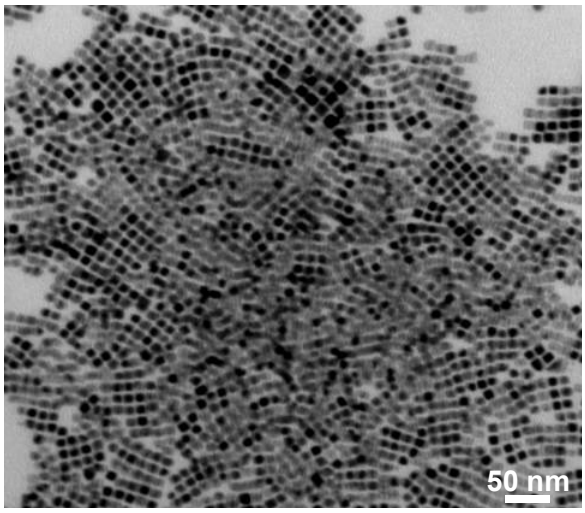

Figure S7. TEM image of the CuPd nanocubes treated by washing and UV light irradiation, showing the partial fusion of the uncapped nanocubes upon TEM electron beam irradiation.

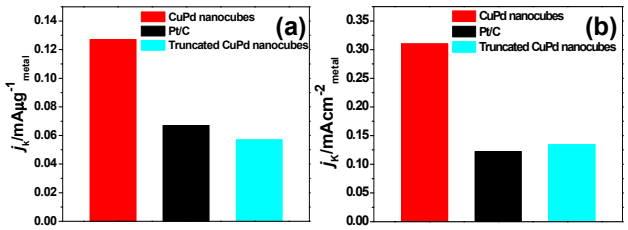

Figure S8. (a) Mass activity and (b) specific activity for these three catalysts, in which the kinetic current densities (j_k) are normalized in reference to the loading amount and ECSA of metal, respectively. All the electrocatalytic measurements were carried out by using a GC RDE at a rotation rate of 1600 rpm and a sweep rate of 10 mV/s at room temperature.

References

1. W. Chen, J. Kim, S. Sun and S. Chen, Electro-oxidation of formic acid catalyzed by FePt nanoparticles. *Phys. Chem. Chem. Phys*., 2006, **8**, 2779–2786.
2. G. Samjeské, A. Miki and M. Osawa, Electrocatalytic Oxidation of Formaldehyde on Platinum under Galvanostatic and Potential Sweep Conditions Studied by Time-Resolved Surface-Enhanced Infrared Spectroscopy. *J. Phys. Chem. C*, 2007, **111**, 15074–15083.
3. R. Rajagopalan and J. O. Iroh, A One-Step Electrochemical Synthesis of Polyaniline–Polypyrrole Composite Coatings on Carbon Fibers. *Electrochim. Acta*, 2002, **47**, 1847–1855.
4. Y. Wei, X. Tang, Y. Sun and W. W. Focke, A Study of the Mechanism of Aniline Polymerization. *J. Polym. Sci., Part A: Polym. Chem*., 1989, **27**, 2385–2396.